Acta Cryst E CRYSTALLOGRAPHIC COMMUNICATIONS

ISSN 2056-9890

Crystal structure of 2,3-dimethylmaleic anhydride: continuous chains of electrostatic attraction

Ren A. Wiscons,[a]* Matthias Zeller[b] and Jesse L. C. Rowsell[a]‡

[a]Department of Chemistry and Biochemistry, Oberlin College, Oberlin, Ohio 44074, USA, and [b]Department of Chemistry, Youngstown State University, Youngstown, Ohio 44555, USA. *Correspondence e-mail: Ren.Wiscons@oberlin.edu

Received 17 June 2015
Accepted 13 July 2015

Edited by G. Smith, Queensland University of Technology, Australia

‡ Dr Jesse Rowsell passed away on January 30, 2015.

Keywords: crystal structure; maleic anhydride; carbonyl–carbonyl interactions

CCDC reference: 1412475
Supporting information: this article has supporting information at journals.iucr.org/e

In the crystal structure of 2,3-dimethylmaleic anhydride, $C_6H_6O_3$, the closest non-bonding intermolecular distances, between the carbonyl C and O atoms of neighboring molecules, were measured as 2.9054 (11) and 3.0509 (11) Å, which are well below the sum of the van der Waals radii for these atoms. These close contacts, as well as packing motifs similar to that of the title compound, were also found in the crystal structure of maleic anhydride itself and other 2,3-disubstituted maleic anhydrides. Computational modeling suggests that this close contact is caused by strong electrostatic interactions between the carbonyl C and O atoms.

1. Chemical context

Maleic anhydride and its symmetrically 2,3-disubstituted derivatives are standard reagents found in nearly all chemical stockrooms due to their importance as metal-organic framework post-synthetic modifiers (Wang & Cohen, 2009), biomolecule denaturation catalysts (Puigserver & Desnuelle, 1975), synthesis reagents (Moad *et al.*, 2003), and temperature and pH-reversible co-polymer grafts (Gao *et al.*, 2009). Although they are seemingly ubiquitous, comparisons of interactions in the solid state of maleic anhydride (Lutz, 2001) and its disubstituted derivatives have not been discussed. Determination of the structure of the title compound, 2,3-dimethylmaleic anhydride by single-crystal X-ray diffraction was completed and is reported herein. Computational modeling was also used to determine the intermolecular interactions present in the title compound as well as in other 2,3-disubstituted derivatives.

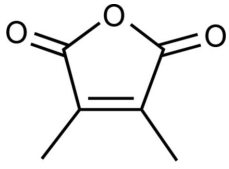

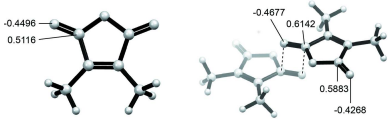

2. Structural commentary

The title compound 2,3-dimethylmaleic anhydride (Fig. 1) is a 5-membered cyclic anhydride with a double bond between carbon atoms C2 and C3. The double bond locks the molecule in a planar conformation and stabilizes the acid anhydride against hydration. The lengths of the C—C single bonds between C1 and C2, and C3 and C4 are 1.4841 (11) and 1.4848 (11) Å, respectively, and that of the C=C bond between C2 and C3 is 1.3420 (12) Å, suggesting that the alkene region of the molecule is not delocalized with the

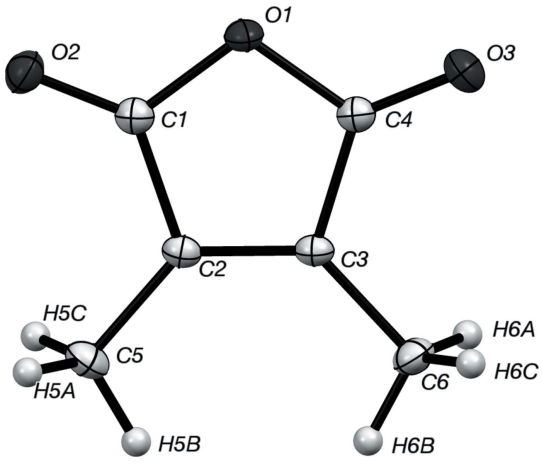

Figure 1
Displacement ellipsoid representation of one molecule of 2,3-dimethylmaleic anhydride, with non-H atoms drawn at the 50% probability level.

carbonyl groups and that the molecule is non-aromatic. The dipole moment of a molecule in the gas phase was calculated as 4.8999 D from DFT B3LYP with a 6-311G(d,p) basis set using *GUUSSIAN03* (Frisch *et al.*, 2004). All bond lengths and angles are consistent with the molecular structure of unsubstituted maleic anhydride (Lutz, 2001).

3. Supramolecular features

In the title compound, close intermolecular carbonyl–carbonyl contacts with $d(^{\delta+}C\cdots^{\delta-}O)$ ranging from 2.9054 (11) to 3.0509 (11) Å in length are present, which is well below the sum of the carbon and oxygen van der Waals radii of 3.22 Å (Bondi, 1964), suggesting a strong attractive interaction between these two atoms. Close carbonyl–carbonyl interactions, in which $d(^{\delta+}C\cdots^{\delta-}O)$ is < 3.6 Å, persist in 15% of carbonyl-substituted small molecule crystal structures surveyed from the Cambridge Structural Database (CSD) by Allen and colleagues in 1998 (Allen *et al.*, 1998). Three carbonyl–carbonyl approach geometries, characterized by specific ranges in angles between the van der Waals radius-overlapped ketonic carbon and oxygen nuclei, were found to describe 71.2% (945 structures) of the observed interactions in the 1,328 crystal structures identified as having close carbonyl–carbonyl contacts: the anti-parallel, perpendicular, and sheared parallel motifs (Fig. 2). Orthogonality of the interacting ketonic nuclei was found to be correlated with multiplicity using *ab initio* calculations to quantify interaction strength (Allen *et al.*, 1998). Doubly C···O connected anti-parallel carbonyl–carbonyl interactions (Fig. 2*a*) approached strengths of −22.3 kJ mol^{-1}, which is competitive with weak-to-medium-strength classical hydrogen bonds, while singly C···O connected perpendicular (Fig. 2*b*) and sheared parallel interactions (Fig. 2*c*) were found to have interaction strengths reaching −7.6 kJ mol^{-1}, which is on a par with strong aromatic stacking interactions (Allen *et al.*, 1998). In addition to the interaction multiplicity, the anti-parallel geometry is strengthened by π–π interactions, lengthening the mean

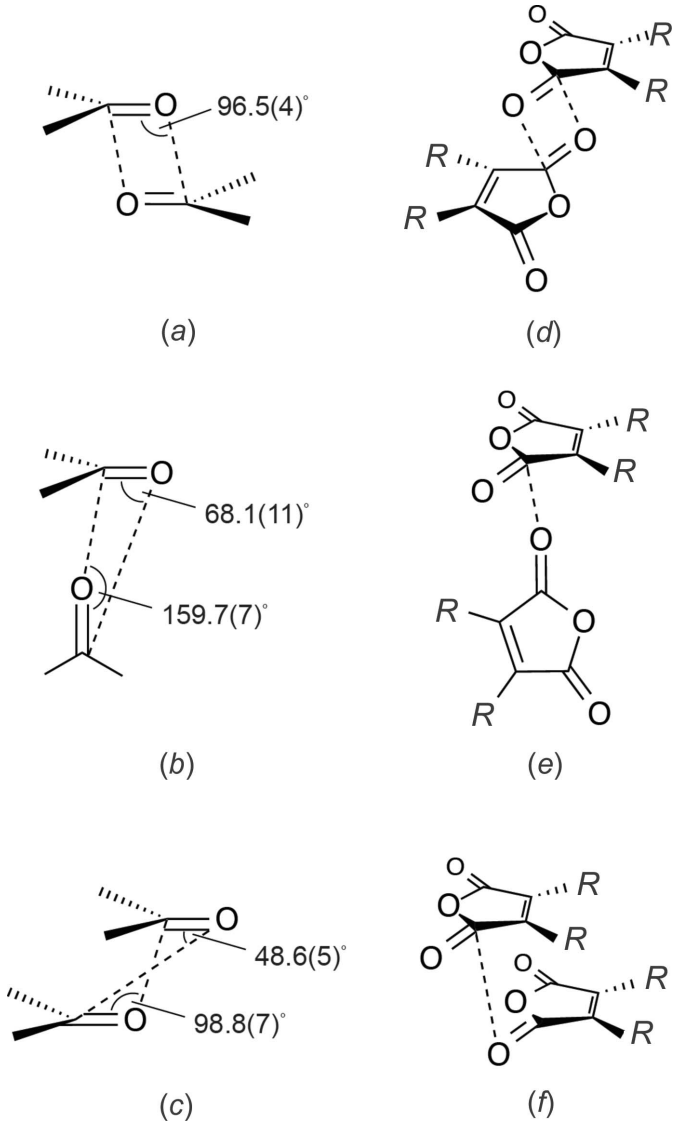

Figure 2
Three carbonyl–carbonyl interaction geometries adapted from Allen *et al.* (1998): (*a*) anti-parallel, (*b*) perpendicular, (*c*) sheared parallel. The three carbonyl–carbonyl geometries as they apply to substituted maleic anhydrides: (*d*) anti-parallel, (*e*) perpendicular, (*f*) sheared parallel.

separation distance between carbonyl–carbonyl contacts relative to those observed in singly connected geometries.

A survey of thirteen previously determined 2,3-disubstituted maleic anhydride crystal structures demonstrates the persistence of the unsubstituted maleic anhydride's carbonyl–carbonyl contacts against steric and electrostatic perturbation (CSD, accessed June 2015; Groom & Allen, 2014). These 2,3-disubstituted maleic anhydride crystal structures and 2,3-dimethylmaleic anhydride were characterized in the context of the parameters described by Allen *et al.* (Table 1 to 3). Computational modeling of electrostatic potential and optimized geometric configurations in homomolecular maleic anhydride complexes suggest that non-covalent carbonyl–carbonyl interactions further polarize the interacting nuclei, reinforcing the electrostatic attraction, while also polarizing the neighboring anhydride carbonyl, and propagating the

Table 1
Anti-parallel interactions (D, Å, °) in di-substituted maleic anhydrides and the intermolecular carbonyl C—O distances in their crystal structures.

Molecule	CSD refcode	δ+ C, δ− C	*d*(C···O)	<*C*═O···C
3,4-bis(2,5-dimethylthien-3-yl)furan-2,5-dione	NOYGEN	0.6603, −0.4326	3.063, 3.063	94.98, 94.98
bicyclo(2.2.1)hepta-2,5-diene-2,3-dicarboxylic anhydride	DAJXIV	0.6565, −0.4329	3.088, 3.927	135.40, 85.90
2,3-diphenylmaleic anhydride	YUYMIO	0.6184, −0.4425	3.575, 3.843	75.83, 63.55
4,5,6,7-tetrahydroisobenzofuran-1,3-dione	NADCOL	0.5666, −0.4474	3.108, 3.191	87.26, 83.39
dimethylmaleic anhydride	this work	0.5116, −0.4496	3.220, 3.259	100.86, 98.90
dichloromaleic anhydride	LIZCOM	0.2166, −0.3742	3.211, 3.219	103.01, 102.55

Table 2
Perpendicular interactions (D, Å, °) in di-substituted maleic anhydrides and the intermolecular carbonyl C—O distances in their crystal structures.

Molecule	CSD refcode	δ+ C, δ− O	*d*(C···O)	<*C*═O···C
bicyclo(2.2.1)hepta-2,5-diene-2,3-dicarboxylic anhydride	DAJXIV	0.6565, −0.4329	3.140, 4.747	137.15, 50.35
3-benzyl-4-phenylfuran-2,5-dione	GUSHOS	0.6410, −0.4266	2.872, 4.257	134.72, 59.61
2,3-diphenylmaleic anhydride	YUYMIO	0.6184, −0.4425	2.913, 3.583	115.98, 80.11
4,5,6,7-tetrahydroisobenzofuran-1,3-dione	NADCOL	0.5666, −0.4474	2.957, 4.360	156.23, 68.51
4,5,6,7-tetrahydroisobenzofuran-1,3-dione	NADCOL	0.5666, −0.4474	3.148, 4.143	124.42, 91.05
dimethylmaleic anhydride	This work	0.5116, −0.4496	2.905, 4.351	152.88, 66.53
dimethylmaleic anhydride	This work	0.5116, −0.4496	3.080, 4.258	130.02, 67.42
4-(4-fluorophenyl)-3-hydroxymaleic anhydride	VEYNIX	0.2632, −0.4579	3.086, 4.271	119.16, 59.94
dichloromaleic anhydride	LIZCOM	0.2166, −0.3742	2.888, 4.346	149.52, 63.38
dichloromaleic anhydride	LIZCOM	0.2166, −0.3742	3.011, 4.275	133.18, 64.81

Table 3
Sheared parallel interactions (D, Å, °) in di-substituted maleic anhydrides and the intermolecular carbonyl C—O distances in their crystal structures.

Molecule	CSD entry code	δ+ C, δ− C	*d*(C···O)	<*C*═O···C
bicyclo(2.2.2)octa-2,5-diene-2,3-dicarboxylic anhydride	GIQRAZ	0.6408, −0.4410	3.184, 4.092	107.62, 63.77
acenaphthylene-1,2-dicarboxylic acid anhydride	KECPIR	0.6385, −0.4422	3.242, 4.030	102.25, 64.70
2-(1,2-dimethylindol-3-yl)-3-(1-propenyl)maleic anhydride	FARQUL	0.5945, −0.4398	3.243, 4.027	92.18, 55.81
bicyclo(2.2.1)hept-2-ene-2,3-dicarboxylic anhydride	DAJXOB	0.5930, −0.4302	3.434, 3.498	87.57, 81.57
2-phenylmaleic anhydride	ZIVKOE	0.4665, −0.4373	3.847, 4.151	83.27, 97.93

carbonyl–carbonyl interactions. The shortest contacts between any two non-H atoms of two molecules are those between the two carbonyl oxygens and the carbonyl C atoms of neighboring molecules. Both anti-parallel and perpendicular motifs are present in the crystal structure (Fig. 3*a*). Though the attraction strength for anti-parallel interactions is predicted to be greater than that of the perpendicular motif (Allen *et al.*, 1998), the shortest two contacts belong to the perpendicular interactions of O2 and O1 with $d(^{\delta+}\mathrm{C}\cdots^{\delta-}\mathrm{O})$ = 2.9054 (11) Å and a C═O···C angle of 152.88 (6)° for C1═O2···C4^{iii}, and $d(^{\delta+}\mathrm{C}\cdots^{\delta-}\mathrm{O})$ = 3.0509 (11) Å and a C═O···C angle of 143.24 (6)° for C4═O3···C2^{i} [symmetry code: (i) $-x, y+\frac{1}{2}, -z+\frac{3}{2}$, (iii) $-x+\frac{1}{2}, y-\frac{1}{2}, z$]. The two anti-parallel interactions are arranged pairwise between the two carbonyls rather than between carbonyls of the same type (*i.e.*, they are not related by inversion symmetry) and they have $d(^{\delta+}\mathrm{C}\cdots^{\delta-}\mathrm{O})$ values of 3.220 (11) and 3.259 (11) Å and C═O···C angles of 100.86 (5) and 98.89 (5) for C1═O2···C4^{iv} and C4═O3···C2^{v}, respectively [symmetry codes: (iv) $x+\frac{1}{2}, y, -z+\frac{3}{2}$; (v) $x-\frac{1}{2}, y, -z+\frac{3}{2}$]. The greater $d(^{\delta+}\mathrm{C}\cdots^{\delta-}\mathrm{O})$ value for the anti-parallel motif relative to the perpendicular motif may be attributed to the π–π interactions between the doubly connected carbonyl groups that accompany the $^{\delta+}\mathrm{C}\cdots^{\delta-}\mathrm{O}$ interactions.

The perpendicular interactions and pairwise anti-parallel interactions connect neighboring molecules to form several interaction motifs (Fig. 3). Each 2,3-dimethylmaleic anhydride molecule participates in four perpendicular interactions, of which each two are symmetry equivalent: as an electron-density acceptor (through the carbonyl C atom) in two of the four interactions and in the other two as an electron-density donor (through the carbonyl O atom). The perpendicular carbonyl–carbonyl interactions associated with both the 2.9054 (11) and 3.0509 (11) Å $^{\delta+}\mathrm{C}\cdots^{\delta-}\mathrm{O}$ distances give rise to pleated chains of 2,3-dimethylmaleic anhydride molecules that extend parallel to the *b*-axis. There are two parallel chains that arise from the two perpendicular interactions with the 2.9054 (11) and 3.0509 (11) Å $^{\delta+}\mathrm{C}\cdots^{\delta-}\mathrm{O}$ separations (C1═O2···C4^{iii} and C4═O3···C2^{i}; Fig. 3*a*). The interactions join parallel chains and combined they create layers perpendicular to the *c*-axis direction. Molecules within these layers are further connected through the pairwise anti-parallel carbonyl interactions and π-stacking, as well as C—H···O interactions between methyl atom H6*A* and atom O1 (Table 4). Only weak intermolecular interactions are found

Table 4
Hydrogen-bond geometry (Å, °).

D—H···*A*	*D*—H	H···*A*	*D*···*A*	*D*—H···*A*
C6—H6*A*···O1^{i}	0.98	2.68	3.5004 (12)	142
C6—H6*B*···O3^{ii}	0.98	2.69	3.5445 (13)	146

Symmetry codes: (i) $-x, y+\frac{1}{2}, -z+\frac{3}{2}$; (ii) $x, -y+\frac{1}{2}, z+\frac{1}{2}$.

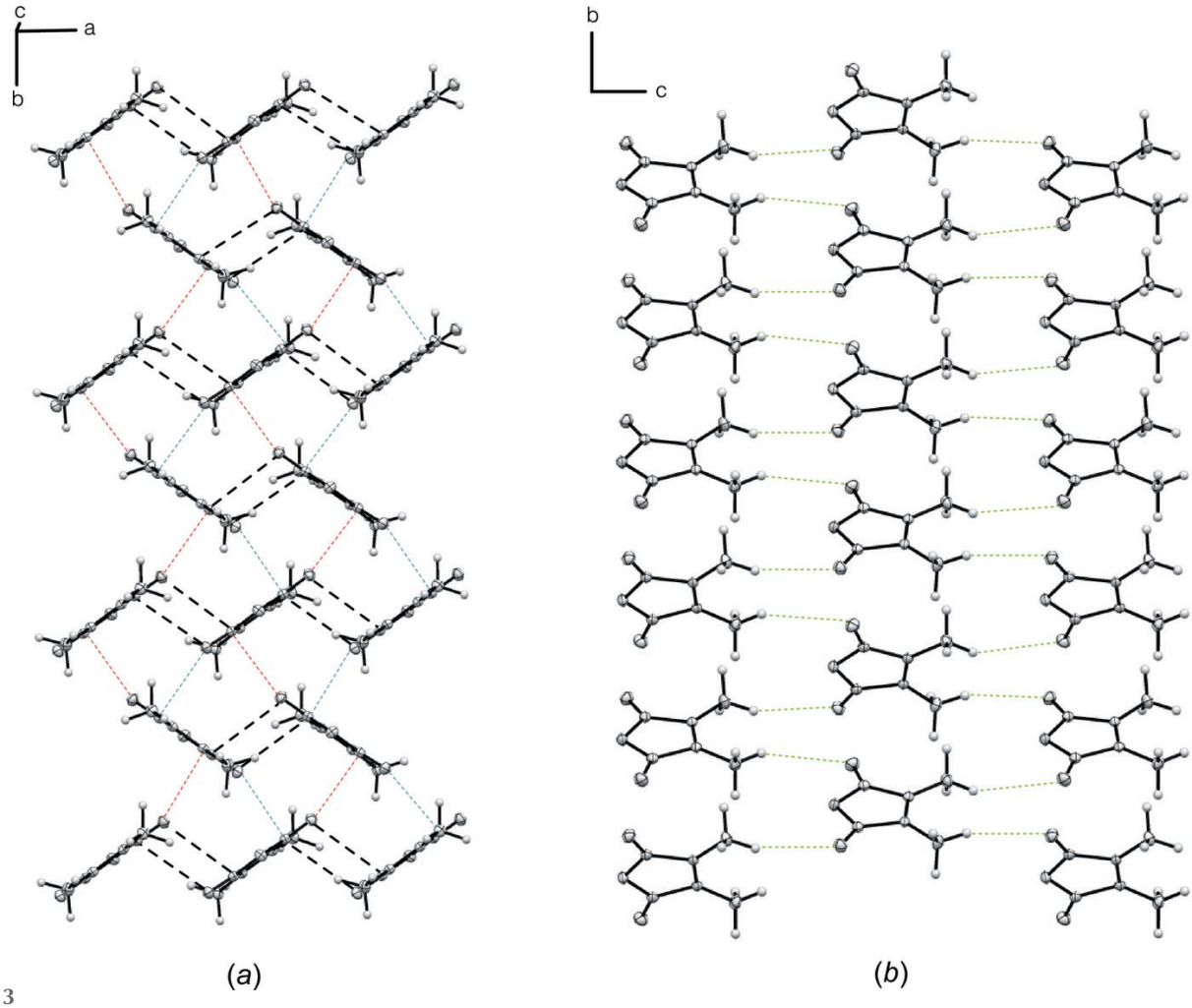

Figure 3
Motifs that arise from non-covalent interactions in 2,3-dimethylmaleic anhydride: (*a*) perpendicular C···O interactions (red and blue for C1═O2···C4^{iii} and C4═O3···C2^{i} interactions respectively) and anti-parallel carbonyl interactions (black, representing C1═O2···C4^{iv} and C4═O3···C2^{v}, respectively), (*b*) weak C—H···O interactions (green) between sheets (weak C—H···O interactions within sheets have been omitted for clarity). Symmetry codes: (iii) $-x+\frac{1}{2}, y-\frac{1}{2}, z$; (iv) $x+\frac{1}{2}, y, -z+\frac{3}{2}$; (v) $x-\frac{1}{2}, y, -z+\frac{3}{2}$. For other codes, see Table 4.

between parallel layers of 2,3-dimethylmaleic anhydride molecules, the most pronounced one being between methyl atom H6*B* and atom O3 (Fig. 3*b*).

4. Computational modeling

To better understand the intermolecular interactions that allow the close contact between the carbonyl C atom and the carbonyl O atom, the anti-parallel carbonyl–carbonyl interaction between two molecules of 2,3-dimethylmaleic anhydride was modeled computationally. The perpendicular carbonyl interaction is not a geometric minimum in the gas phase and thus was not modeled due to the unknown contributions from additional solid-state interactions. Geometry optimizations were performed for one molecule of 2,3-dimethylmaleic anhydride and a dimer of 2,3-dimethylmaleic anhydride using DFT B3LYP with the 6-31G(d) basis set using *GAUSSIAN03* (Frisch *et al.*, 2004). Geometry optimization of the two-molecule complex revealed a strong interaction between the carbonyl O atom and carbonyl C atom with a short $d(^{\delta+}C\cdots{}^{\delta-}O)$ of 3.178 Å, which is consistent with the value from the crystal structure [3.220 (11) Å] and is below the sum of the van der Waals radii for O and C (3.22 Å). The Mulliken atomic charges of the carbonyl O atom (−0.4496) and carbonyl C atom (+0.5116) suggest that this interaction is likely electrostatic in nature (Fig. 4*a*). Comparison of the computed Mulliken atomic charges of the two-molecule complex with that of a single molecule indicates that both the carbonyl C atom (+0.6142) and carbonyl O atom (−0.4677) atoms participating in the anti-parallel interaction (Fig. 4*b*) are further polarized relative to the free molecule (Fig. 4*a*). More interestingly, in the two-molecule complex, even the carbonyl C atom not directly involved in the electrostatic attraction is further polarized, with a calculated Mulliken atomic charge of +0.5883 versus +0.5116 in the single-molecule model. These data suggest that the carbon–oxygen electrostatic interaction on one end of the anhydride draws electron density from the carbonyl C atom on the other and enables 2,3-dimethylmaleic anhydride to better interact with a neighboring carbonyl O atom.

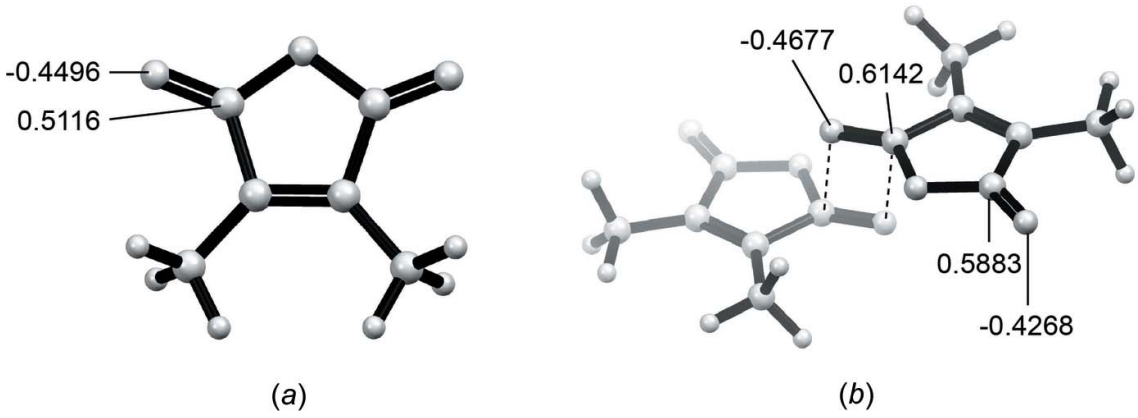

Figure 4
Optimized structures of the single molecule model (*a*) and the 2,3-dimethylmaleic anhydride dimer with a separation distance of 3.187 Å and (*b*), with indicated Mulliken atomic charges.

Induced polarization reinforces the overall strength of the carbonyl–carbonyl network within the crystal structure both between molecules, forming chains through perpendicular interactions, and between anti-parallel chains, forming sheets. Based on these calculations, it can be predicted that with increased polarization of the carbonyl carbon and oxygen nuclei, the strength of the intermolecular interaction between carbonyls would increase and the shortest contact between the interacting nuclei would decrease. Additional inductive effects of dimerization include an increase in the average Mulliken atomic charge of the methyl H atoms (+0.1859) relative to that of the free molecule (+0.1499), which would have the effect of slightly strengthening the weak C—H···O attractions that connect layers of molecules associated through the carbonyl–carbonyl interactions.

5. Database survey

The Mulliken atomic charges for thirteen 2,3-disubstituted maleic anhydrides found in the CSD were calculated and their crystal structures analyzed for $d(^{\delta+}C\cdots^{\delta-}O)$ and geometries (Tables 1, 2 and 3). The expected trend is most apparent amongst the set of sheared-parallel carbonyl–carbonyl interactions in which the participating nuclei are isolated from additional non-covalent interactions, unlike those found in anti-parallel and perpendicular motifs. This trend supports the prediction that $d(^{\delta+}C\cdots^{\delta-}O)$ decreases with increased carbonyl polarization. The expected trend in anti-parallel $d(^{\delta+}C\cdots^{\delta-}O)$ is disrupted by YUYMIO, a 2,3-diphenylmaleic anhydride, whose packing is also guided by edge-face aromatic interactions [d(C—H···centroid] of 3.187 Å). Because of the packing frustration presented by these two competing interactions in 2,3-diphenylmaleic anhydride, its disruption of the $d(^{\delta+}C\cdots^{\delta-}O)$ trend may be disregarded. These data suggest that C2 and C3 functionalization can affect the carbonyl–carbonyl interaction distance for a particular interaction geometry (anti-parallel, perpendicular, and sheared-parallel) through polarization of the carbonyl group. The persistence of the major interactions in maleic acid anhydrides indicates that electrostatic distribution and intermolecular interaction-induced polarization of the anhydride's carbonyls contribute strongly to the molecular packing and are competitive with other common supramolecular moieties, such as hydrogen-bonding and aromatic stacking.

6. Synthesis and crystallization

Crystals were grown by dissolving 2 g of 2,3-dimethylmaleic anhydride in 100 mL of deionized H_2O at 373 K. Once dissolved, the solution was slowly cooled to 277 K, crystallizing colorless plates.

Table 5
Experimental details.

Crystal data	
Chemical formula	$C_6H_6O_3$
M_r	126.11
Crystal system, space group	Orthorhombic, *Pbca*
Temperature (K)	100
a, *b*, *c* (Å)	10.4087 (18), 8.5848 (15), 13.095 (2)
V (Å^3)	1170.1 (3)
Z	8
Radiation type	Mo $K\alpha$
μ (mm^{-1})	0.12
Crystal size (mm)	0.50 × 0.31 × 0.19
Data collection	
Diffractometer	Bruker APEXII CCD
Absorption correction	Multi-scan (*SADABS*; Bruker, 2013)
T_{min}, T_{max}	0.643, 0.746
No. of measured, independent and observed [$I > 2\sigma(I)$] reflections	16692, 1856, 1688
R_{int}	0.031
(sin $\theta/\lambda)_{max}$ (Å^{-1})	0.735
Refinement	
$R[F^2 > 2\sigma(F^2)]$, $wR(F^2)$, S	0.037, 0.101, 1.07
No. of reflections	1856
No. of parameters	84
H-atom treatment	H-atom parameters constrained
$\Delta\rho_{max}$, $\Delta\rho_{min}$ (e Å^{-3})	0.53, −0.19

Computer programs: *APEX2* and *SAINT* (Bruker, 2013), *SHELXS97* (Sheldrick, 2008), *SHELXL2014* (Sheldrick, 2015), *SHELXLE* (Hübschle *et al.*, 2011), *Mercury* (Macrae *et al.*, 2008) and *publCIF* (Westrip, 2010).

7. Refinement

Crystal data, data collection and structure refinement details are summarized in Table 5. H atoms were positioned geometrically and constrained to ride on their parent atoms, with carbon–hydrogen bond distances of 0.95 Å for C—H, and 0.98 Å for CH_3 moieties, respectively. Methyl H atoms were allowed to rotate but not to tip to best fit the experimental electron density. U_{iso}(H) values were set to a multiple of U_{eq}(C) with 1.5 for CH_3 and 1.2 for C—H.

Acknowledgements

The X-ray diffractometer was funded by NSF grant 0087210, Ohio Board of Regents grant CAP-491, and by Youngstown State University. The authors would like to thank Oberlin College for funding this research.

References

Allen, F. H., Baalham, C. A., Lommerse, J. P. M. & Raithby, P. R. (1998). *Acta Cryst.* B**54**, 320–329.
Bondi, A. (1964). *J. Phys. Chem.* **68**, 441–451.
Bruker (2013). *APEX2*, *SADABS* and *SAINT*. Bruker AXS Inc., Madison, Wisconsin, USA.
Frisch, M. J., Trucks, G. W., Schlegel, H. B., Scuseria, G. E., Robb, M. A., Cheeseman, J. R., Montgomery, J. A. Jr, Vreven, T., Kudin, K. N., Burant, J. C., Millam, J. M., Iyengar, S. S., Tomasi, J., Barone, V., Mennucci, B., Cossi, M., Scalmani, G., Rega, N., Petersson, G. A., Nakatsuji, H., Hada, M., Ehara, M., Toyota, K., Fukuda, R., Hasegawa, J., Ishida, M., Nakajima, T., Honda, Y., Kitao, O., Nakai, H., Klene, M., Li, X., Knox, J. E., Hratchian, H. P., Cross, J. B., Bakken, V., Adamo, C., Jaramillo, J., Gomperts, R., Stratmann, R. E., Yazyev, O., Austin, A. J., Cammi, R., Pomelli, C., Ochterski, J. W., Ayala, P. Y., Morokuma, K., Voth, G. A., Salvador, P., Dannenberg, J. J., Zakrzewski, V. G., Dapprich, S., Daniels, A. D., Strain, M. C., Farkas, O., Malick, D. K., Rabuck, A. D., Raghavachari, K., Foresman, J. B., Ortiz, J. V., Cui, Q., Baboul, A. G., Clifford, S., Cioslowski, J., Stefanov, B. B., Liu, G., Liashenko, A., Piskorz, P., Komaromi, I., Martin, R. L., Fox, D. J., Keith, T., Al-Laham, M. A., Peng, C. Y., Nanayakkara, A., Challacombe, M., Gill, P. M. W., Johnson, B., Chen, W., Wong, M. W., Gonzalez, C. & Pople, J. A. (2004). *GAUSSIAN03*. Gaussian Inc., Wallingford, CT, USA.
Gao, M., Jia, X., Kuang, G., Li, Y., Liang, D. & Wei, Y. (2009). *Macromolecules*, **42**, 4273–4281.
Groom, C. R. & Allen, F. H. (2014). *Angew. Chem. Int. Ed.* **53**, 662–671.
Hübschle, C. B., Sheldrick, G. M. & Dittrich, B. (2011). *J. Appl. Cryst.* **44**, 1281–1284.
Lutz, M. (2001). *Acta Cryst.* E**57**, o1136–o1138.
Macrae, C. F., Bruno, I. J., Chisholm, J. A., Edgington, P. R., McCabe, P., Pidcock, E., Rodriguez-Monge, L., Taylor, R., van de Streek, J. & Wood, P. A. (2008). *J. Appl. Cryst.* **41**, 466–470.
Moad, G., Mayadunne, R. T. A., Rizzardo, E., Skidmore, M. & Thang, S. H. (2003). *Macromol. Symp.* **192**, 1–12.
Puigserver, A. & Desnuelle, P. (1975). *Proc. Natl Acad. Sci. USA*, **72**, 2442–2445.
Sheldrick, G. M. (2008). *Acta Cryst.* A**64**, 112–122.
Sheldrick, G. M. (2015). *Acta Cryst.* C**71**, 3–8.
Wang, Z. & Cohen, S. M. (2009). *Chem. Soc. Rev.* **38**, 1315–1329.
Westrip, S. P. (2010). *J. Appl. Cryst.* **43**, 920–925.

supporting information

Acta Cryst. (2015). E**71**, 950-955 [https://doi.org/10.1107/S2056989015013419]

Crystal structure of 2,3-dimethylmaleic anhydride: continuous chains of electrostatic attraction

Ren A. Wiscons, Matthias Zeller and Jesse L. C. Rowsell

Computing details

Data collection: *APEX2* (Bruker, 2013); cell refinement: *SAINT* (Bruker, 2013); data reduction: *SAINT* (Bruker, 2013); program(s) used to solve structure: *SHELXS97* (Sheldrick, 2008); program(s) used to refine structure: *SHELXL2014* (Sheldrick, 2015) and *SHELXLE* (Hübschle *et al.*, 2011); molecular graphics: *Mercury* (Macrae *et al.*, 2008); software used to prepare material for publication: *publCIF* (Westrip, 2010).

3,4-Dimethylfuran-2,5-dione

Crystal data

$C_6H_6O_3$
M_r = 126.11
Orthorhombic, *Pbca*
a = 10.4087 (18) Å
b = 8.5848 (15) Å
c = 13.095 (2) Å
V = 1170.1 (3) Å^3
Z = 8
$F(000)$ = 528
D_x = 1.432 Mg m^{-3}
Mo $K\alpha$ radiation, λ = 0.71073 Å
Cell parameters from 4877 reflections
θ = 3.1–31.3°
μ = 0.12 mm^{-1}
T = 100 K
Plate, colourless
0.50 × 0.31 × 0.19 mm

Data collection

Bruker APEXII CCD diffractometer
Radiation source: fine focus sealed tube
Graphite monochromator
ω and phi scans
Absorption correction: multi-scan (SADABS; Bruker, 2013)
T_{min} = 0.643, T_{max} = 0.746
16692 measured reflections
1856 independent reflections
1688 reflections with $I > 2\sigma(I)$
R_{int} = 0.031
θ_{max} = 31.5°, θ_{min} = 3.5°
h = −15→15
k = −12→12
l = −19→19

Refinement

Refinement on F^2
Least-squares matrix: full
$R[F^2 > 2\sigma(F^2)]$ = 0.037
$wR(F^2)$ = 0.101
S = 1.07
1856 reflections
84 parameters
0 restraints
Primary atom site location: structure-invariant direct methods
Secondary atom site location: difference Fourier map
Hydrogen site location: inferred from neighbouring sites
H-atom parameters constrained
$w = 1/[\sigma^2(F_o^2) + (0.0563P)^2 + 0.342P]$ where $P = (F_o^2 + 2F_c^2)/3$
$(\Delta/\sigma)_{max}$ = 0.001
$\Delta\rho_{max}$ = 0.53 e Å^{-3}
$\Delta\rho_{min}$ = −0.19 e Å^{-3}

Special details

Geometry. All e.s.d.'s (except the e.s.d. in the dihedral angle between two l.s. planes) are estimated using the full covariance matrix. The cell e.s.d.'s are taken into account individually in the estimation of e.s.d.'s in distances, angles and torsion angles; correlations between e.s.d.'s in cell parameters are only used when they are defined by crystal symmetry. An approximate (isotropic) treatment of cell e.s.d.'s is used for estimating e.s.d.'s involving l.s. planes.

Fractional atomic coordinates and isotropic or equivalent isotropic displacement parameters (Å²)

	x	*y*	*z*	U_{iso}*/U_{eq}
C1	0.21013 (8)	0.04947 (9)	0.74377 (6)	0.01397 (17)
C2	0.16580 (8)	0.09029 (9)	0.84811 (6)	0.01289 (17)
C3	0.06175 (8)	0.18143 (9)	0.83852 (6)	0.01265 (17)
C4	0.03516 (8)	0.20010 (9)	0.72780 (6)	0.01341 (17)
C5	0.23380 (9)	0.03114 (10)	0.93985 (7)	0.01846 (19)
H5A	0.2334	−0.0830	0.9392	0.028*
H5B	0.1902	0.0687	1.0015	0.028*
H5C	0.3227	0.0687	0.9394	0.028*
C6	−0.02176 (9)	0.25635 (10)	0.91611 (7)	0.01814 (19)
H6A	−0.0139	0.3698	0.9108	0.027*
H6B	0.0048	0.2229	0.9845	0.027*
H6C	−0.1113	0.2258	0.9043	0.027*
O1	0.12815 (6)	0.11870 (7)	0.67262 (5)	0.01582 (16)
O2	0.29960 (6)	−0.02770 (8)	0.71646 (5)	0.01983 (17)
O3	−0.04983 (6)	0.26794 (8)	0.68539 (5)	0.01860 (16)

Atomic displacement parameters (Å²)

	U^{11}	U^{22}	U^{33}	U^{12}	U^{13}	U^{23}
C1	0.0154 (4)	0.0128 (3)	0.0137 (4)	−0.0016 (3)	0.0001 (3)	−0.0002 (3)
C2	0.0145 (4)	0.0126 (3)	0.0115 (3)	−0.0023 (3)	−0.0003 (3)	0.0003 (3)
C3	0.0151 (4)	0.0125 (3)	0.0103 (3)	−0.0020 (3)	0.0005 (2)	−0.0004 (2)
C4	0.0149 (4)	0.0125 (3)	0.0129 (3)	−0.0015 (3)	0.0005 (3)	−0.0004 (3)
C5	0.0194 (4)	0.0210 (4)	0.0150 (4)	−0.0005 (3)	−0.0042 (3)	0.0030 (3)
C6	0.0185 (4)	0.0208 (4)	0.0151 (4)	0.0014 (3)	0.0037 (3)	−0.0026 (3)
O1	0.0192 (3)	0.0177 (3)	0.0106 (3)	0.0027 (2)	0.0002 (2)	−0.0011 (2)
O2	0.0188 (3)	0.0195 (3)	0.0212 (3)	0.0035 (2)	0.0035 (2)	−0.0018 (2)
O3	0.0186 (3)	0.0191 (3)	0.0181 (3)	0.0011 (2)	−0.0039 (2)	0.0023 (2)

Geometric parameters (Å, º)

C1—O2	1.1976 (10)	C4—O1	1.3955 (10)
C1—O1	1.3963 (10)	C5—H5A	0.9800
C1—C2	1.4841 (11)	C5—H5B	0.9800
C2—C3	1.3420 (12)	C5—H5C	0.9800
C2—C5	1.4840 (11)	C6—H6A	0.9800
C3—C6	1.4837 (11)	C6—H6B	0.9800
C3—C4	1.4848 (11)	C6—H6C	0.9800
C4—O3	1.1959 (10)		

O2—C1—O1	120.76 (8)	C2—C5—H5B	109.5
O2—C1—C2	130.35 (8)	H5A—C5—H5B	109.5
O1—C1—C2	108.90 (7)	C2—C5—H5C	109.5
C3—C2—C5	131.32 (8)	H5A—C5—H5C	109.5
C3—C2—C1	107.60 (7)	H5B—C5—H5C	109.5
C5—C2—C1	121.08 (7)	C3—C6—H6A	109.5
C2—C3—C6	131.41 (8)	C3—C6—H6B	109.5
C2—C3—C4	107.74 (7)	H6A—C6—H6B	109.5
C6—C3—C4	120.84 (7)	C3—C6—H6C	109.5
O3—C4—O1	121.09 (8)	H6A—C6—H6C	109.5
O3—C4—C3	130.09 (8)	H6B—C6—H6C	109.5
O1—C4—C3	108.80 (7)	C4—O1—C1	106.95 (6)
C2—C5—H5A	109.5		

O2—C1—C2—C3	179.19 (8)	C2—C3—C4—O3	177.77 (8)
O1—C1—C2—C3	−0.43 (9)	C6—C3—C4—O3	−1.64 (14)
O2—C1—C2—C5	−1.17 (13)	C2—C3—C4—O1	−0.84 (9)
O1—C1—C2—C5	179.21 (7)	C6—C3—C4—O1	179.75 (7)
C5—C2—C3—C6	0.48 (15)	O3—C4—O1—C1	−178.21 (7)
C1—C2—C3—C6	−179.93 (8)	C3—C4—O1—C1	0.55 (8)
C5—C2—C3—C4	−178.84 (8)	O2—C1—O1—C4	−179.77 (7)
C1—C2—C3—C4	0.75 (9)	C2—C1—O1—C4	−0.10 (8)

Hydrogen-bond geometry (Å, º)

D—H···*A*	*D*—H	H···*A*	*D*···*A*	*D*—H···*A*
C6—H6*A*···O1^{i}	0.98	2.68	3.5004 (12)	142
C6—H6*B*···O3^{ii}	0.98	2.69	3.5445 (13)	146

Symmetry codes: (i) −*x*, *y*+1/2, −*z*+3/2; (ii) *x*, −*y*+1/2, *z*+1/2.